

Figure 3. Upregulation of *HOTAIR* in malignant GISTs. A, TaqMan assay of *HOTAIR* in a panel of GIST specimens ( $n = 52$ ). Results are normalized to internal *GAPDH* expression. Risk categories are indicated below. B, correlation between levels of *HOTAIR* and miR-196a expression detected using TaqMan assay. The Pearson correlation coefficient and  $P$  value are shown. C, correlations between levels of *HOTAIR* expression detected using TaqMan assay and those of *HOXC* genes detected from microarrays. The Pearson correlation coefficients and  $P$  values are shown. D, Kaplan-Meier curves showing the effect of *HOTAIR* expression (high, *HOTAIR/GAPDH*  $\geq 0.0002$ ; low, *HOTAIR/GAPDH*  $< 0.0002$ ) on overall survival among GIST patients. E, TaqMan assay for *HOTAIR* in GIST-T1 cells transfected with control siRNA (siCONT) or siRNA targeting *HOTAIR* (siHOT). F, cell viability assay using GIST-T1 cells transfected with siCONT or siHOT. Cell viabilities were determined 48 hours after transfection. Shown are the means of 8 replications; error bars represent SDs. G, Matrigel invasion assay using GIST-T1 cells transfected with siCONT or siHOT. Shown on the right are the means of 3 random microscopic fields per membrane; error bars represent SDs.

organelle" (Supplementary Tables S12 and S13). These results suggested that *HOTAIR* may modulate transcription of a large number of genes and may have previously unidentified roles in GIST cells.

Finally, we sought to clarify the biologic relationship between miR-196a, *HOTAIR*, and *HOXC* genes. We first tested whether upregulation of miR-196a is a downstream effect of *HOTAIR* dysregulation, or vice versa. We found that inhibition

**Table 4.** HOTAIR expression is associated with poor clinical outcome in GIST patients

HOTAIR/GAPDH	Outcome					
	Survival	Death	HR (95% CI)	P	HR <sup>a</sup> (95% CI)	P
<0.0002	26	2				
≥0.0002	7	4	3.8 (0.7–21.2)	0.123	9.0 (1.2–68.9)	0.034

<sup>a</sup>Age and gender adjusted HR.

of miR-196a had no effect on *HOTAIR* expression in GIST-T1 cells, nor did knockdown of *HOTAIR* affect miR-196a expression. This suggested that overexpression of miR-196a or *HOTAIR* is not a simple downstream effect of their dysregulation (Supplementary Fig. S12). By contrast, analysis of the chromatin status in GIST-T1 cells using ChIP-PCR revealed enrichment of trimethylated histone H3 lysine 4 (H3K4me3), a hallmark of active gene transcription, at the transcription start sites of multiple *HOXC* genes and *HOTAIR* (Supplementary Fig. S14). Moreover, we found concurrent overexpression of miR-196a, *HOTAIR*, and *HOXC* genes in other cancer cells, including the KatoIII gastric cancer cell line. By carrying out high-resolution ChIP-seq analysis with the KatoIII cells, we observed significant enrichment of H3K4me3 over a wide range (more than 50 kb) of the *HOXC* cluster, which suggested that an epigenetic mechanism is involved in the dysregulation of this genomic region (Supplementary Fig. S15).

## Discussion

Although the results of recent studies suggest that the gene expression signatures of GISTs are predictive of malignancy and drug sensitivity of the tumors (5, 21), the clinical significance of the miRNA expression signature is not yet fully understood. In this study, we found that upregulation of miR-196a is strongly associated with a high-risk grade, metastasis, and poor prognosis in GIST patients. Furthermore, overexpression of miR-196a is accompanied by upregulation of multiple *HOXC* genes and the metastasis-related lincRNA *HOTAIR*. To our knowledge, this is the first article to show concurrent overexpression of collinear *HOXC* genes and non-coding RNAs in human malignancy.

A number of studies have implicated miR-196a in malignancy, but its role may differ among tumor types. Upregulation of miR-196a is observed in esophageal adenocarcinomas and their precancerous lesions, Barrett's esophagus and dysplasia, which suggests miR-196a is a potential marker of the malignant progression of Barrett's esophagus (22). Strong expression of miR-196a is also associated with a poor prognosis in pancreatic adenocarcinoma and glioblastoma patients (23, 24). In addition, functional analysis showed that expression of miR-196a in esophageal, breast, and endometrial cancer cells promotes proliferation and suppresses apoptosis through downregulation of *ANXA1* (18). These results suggest that miR-196a contributes to oncogenesis in cancer. On the other hand, miR-196a is significantly downregulated in melanoma, and its

reexpression inhibited the invasive behavior of melanoma cells by targeting *HOXC8* (25). Similarly, miR-196a suppressed *HOXC8* and inhibited invasion and metastasis by breast cancer cells (26). Thus miR-196a seems to exert opposite effects in tumors of different origins.

The *HOX* genes are a highly conserved subgroup of the homeobox superfamily, and they play essential roles in a variety of biologic processes, including development, differentiation, apoptosis, and angiogenesis (27). In humans, 4 *HOX* clusters containing 39 *HOX* genes have been identified, and dysregulation of their expression is observed in various malignancies. Although the role of *HOX*s in cancer is not fully understood, its aberrant expression is thought to affect pathways that promote tumorigenesis and metastasis (27). For instance, *HOXC8* mRNA is overexpressed in prostate cancer cells and is associated with tumor cell proliferation and metastasis (28–30). In addition, *HOXC5* and *HOXC8* mRNAs are upregulated in cervical cancer cells (31), and one recent study suggested *HOXC10* plays a key role of in the progression and invasion in cervical cancer (32).

An association between miR-196a and *HOX* expression in cancer has also been reported. Reduced expression of miR-196a in malignant melanoma cells leads to upregulation of *HOXB7* and, in turn, activation of *BMP4*, a major modulator of migration (33). As mentioned above, miR-196a also inhibits invasion and metastasis by downregulating *HOXC8* in melanoma and breast cancer cells (26, 34). Taken together, these results suggest that miR-196a acts as a tumor suppressor by targeting *HOX* genes in these tumor types. By contrast, we show in this study that both the miR-196a and *HOXC* genes are concurrently upregulated in malignant GISTs. Our findings are reminiscent of an earlier report showing that the expression patterns of miRNAs embedded in *HOX* clusters are very similar to those of *HOX* genes during mammalian embryogenesis (35). Global gene expression analysis revealed that expression of multiple putative miR-196a targets, including *ANXA1*, is diminished in GISTs overexpressing miR-196a, whereas their expression is enhanced upon inhibition of miR-196a in cultured GIST-T1 cells. In addition, inhibition of miR-196a in GIST cells overexpressing that miRNA moderately suppressed cell invasion. Taken together, our results indicate that upregulation of *HOXC* genes along with miR-196a may contribute to the malignant potential of GIST.

*HOTAIR* is located within the *HOXC* cluster and encodes a lincRNA known to repress its target genes by directly interacting with histone modification complexes. Epigenetic gene



regulation is closely associated with histone modifications in which di- or trimethylation of histone H3 lysine 4 (H3K4me2 or H3K4me3) is enriched within active gene promoters. In addition, trimethylation of histone H3 lysine 27 (H3K27me3) is a marker of gene silencing. In normal adult fibroblasts, *HOTAIR* suppresses the *HOXD* locus by recruiting the PRC2 complex, which consists of the histone H3K27 methylase EZH2, SUZ12, and EED (20). It was also recently shown that *HOTAIR* serves as a scaffold for multiple repressor complexes, including PRC2 and LSD1/CoREST/REST (36). LSD1 is a demethylase that specifically mediates demethylation of H3K4, leading to repression of the target genes. *HOTAIR* is also strongly implicated in cancer metastasis. In breast cancer cells, *HOTAIR* induces retargeting of the PRC2 complex throughout the genome, which leads to the silencing of multiple tumor suppressor and metastasis suppressor genes (17). Overexpression of *HOTAIR* is also predictive of recurrence in hepatocellular carcinoma patients after liver transplantation (37). We observed that upregulation of *HOTAIR* is closely associated with GIST aggressiveness and metastasis. In addition, functional analysis using GIST-T1 cells showed that RNAi-mediated knockdown of *HOTAIR* suppressed cell invasion. These results strongly suggest that upregulation of *HOTAIR* is one of the mechanisms that promote aggressiveness in GISTs. Interestingly, depletion of *HOTAIR* induced a significant change in the gene expression profile in GIST cells, suggesting that *HOTAIR* may regulate a spectrum of genes other than the previously reported target genes. Further studies, including genome-wide histone modification analysis, may reveal as yet unidentified roles played by *HOTAIR* in the malignant progression of GISTs.

The mechanism underlying upregulation of *HOX* cluster genes and noncoding RNAs in GISTs is intriguing. Our array CGH analysis did not detect chromosomal aberrations in any *HOX* loci, making it unlikely that gene amplification is the cause of their overexpression. However, we found that the transcription start sites of multiple genes in the *HOXC* cluster are marked by an active histone mark, H3K4me3, in GIST-T1 cells. Moreover, high-resolution ChIP-seq analysis revealed

that, in cancer cells, the entire region is significantly enriched with H3K4me3, leading to overexpression of the affected genes. Our results are reminiscent of the recent finding that rearrangement of *MLL* in leukemia induces active histone modifications at the promoters of *HOXA* genes and miR-196b, resulting to their overexpression (38–40). Although such rearrangements are not known in GISTs, further study to clarify the involvement of epigenetic modifiers in malignant GISTs may lead to identification of new therapeutic targets.

Overall, our study has shown that noncoding RNAs encoded in the *HOXC* cluster could be useful predictive markers as well as novel therapeutic targets in malignant GISTs. As miRNAs are well preserved in FFPE specimens (41), miR-196a could be a reliable biomarker for risk assessment. We also provide evidence that *HOTAIR* is significantly upregulated in high-risk GISTs, indicating that this lincRNA also could be a useful biomarker, as well as a novel therapeutic target. Further study of the causes and functions of *HOXC* locus activation in GISTs may provide new strategies for the treatment of GIST patients.

#### Disclosure of Potential Conflicts of Interest

T. Nishida has received a research grant from Novartis Pharma K.K. The remaining authors disclose no conflicts of interest.

#### Acknowledgments

The authors thank Dr. William F. Goldman for editing the manuscript and M. Ashida for technical assistance.

#### Grant Support

This study was supported in part by grants-in-aid for Scientific Research (B) from the Japan Society for Promotion of Science (Y. Shinomura), A3 foresight program from the Japan Society for Promotion of Science (H. Suzuki), a grant-in-aid for the Third-term Comprehensive 10-year Strategy for Cancer Control (M. Toyota, H. Suzuki), a grant-in-aid for Cancer Research from the Ministry of Health, Labor, and Welfare, Japan (M. Toyota, H. Suzuki), and the Takeda Science Foundation (H. Suzuki).

The costs of publication of this article were defrayed in part by the payment of page charges. This article must therefore be hereby marked *advertisement* in accordance with 18 U.S.C. Section 1734 solely to indicate this fact.

Received May 31, 2011; revised December 19, 2011; accepted January 6, 2012; published OnlineFirst January 18, 2012.

#### References

- Shinomura Y, Kinoshita K, Tsutsui S, Hirota S. Pathophysiology, diagnosis, and treatment of gastrointestinal stromal tumors. *J Gastroenterol* 2005;40:775–80.
- Rubin BP, Heinrich MC, Corless CL. Gastrointestinal stromal tumour. *Lancet* 2007;369:1731–41.
- Corless CL, Fletcher JA, Heinrich MC. Biology of gastrointestinal stromal tumors. *J Clin Oncol* 2004;22:3813–25.
- Fletcher CD, Berman JJ, Corless C, Gorstein F, Lasota J, Longley BJ, et al. Diagnosis of gastrointestinal stromal tumors: A consensus approach. *Hum Pathol* 2002;33:459–65.
- Yamaguchi U, Nakayama R, Honda K, Ichikawa H, Hasegawa T, Shitashige M, et al. Distinct gene expression-defined classes of gastrointestinal stromal tumor. *J Clin Oncol* 2008;26:4100–8.
- Igarashi S, Suzuki H, Niinuma T, Shimizu H, Nojima M, Iwaki H, et al. A novel correlation between LINE-1 hypomethylation and the malignancy of gastrointestinal stromal tumors. *Clin Cancer Res* 2010;16:5114–23.
- He L, Hannon GJ. MicroRNAs: small RNAs with a big role in gene regulation. *Nat Rev Genet* 2004;5:522–31.
- Esquela-Kerscher A, Slack FJ. Oncomir-microRNAs with a role in cancer. *Nat Rev Cancer* 2006;6:259–69.
- Croce CM. Causes and consequences of microRNA dysregulation in cancer. *Nat Rev Genet* 2009;10:704–14.
- Calin GA, Croce CM. MicroRNA signatures in human cancers. *Nat Rev Cancer* 2006;6:857–66.
- Choi HJ, Lee H, Kim H, Kwon JE, Kang HJ, You KT, et al. MicroRNA expression profile of gastrointestinal stromal tumors is distinguished by 14q loss and anatomic site. *Int J Cancer* 2010;126:1640–50.
- Haller F, von Heydebreck A, Zhang JD, Gunawan B, Langer C, Ramadori G, et al. Localization- and mutation-dependent microRNA (miRNA) expression signatures in gastrointestinal stromal tumours (GISTs), with a cluster of co-expressed miRNAs located at 14q32.31. *J Pathol* 2010;220:71–86.
- Maruyama R, Choudhury S, Kowalczyk A, Bessarabova M, Beresford-Smith B, Conway T, et al. Epigenetic regulation of cell type-specific expression patterns in the human mammary epithelium. *PLoS Genet* 2011;7:e1001369.
- Suzuki H, Takatsuka S, Akashi H, Yamamoto E, Nojima M, Maruyama R, et al. Genome-wide profiling of chromatin signatures reveals epigenetic regulation of microRNA genes in colorectal cancer. *Cancer Res* 2011;71:5646–58.

15. Taguchi T, Sonobe H, Toyonaga S, Yamasaki I, Shuin T, Takano A, et al. Conventional and molecular cytogenetic characterization of a new human cell line, GIST-T1, established from gastrointestinal stromal tumor. *Lab Invest* 2002;82:663-5.
16. Calin GA, Sevignani C, Dumitru CD, Hyslop T, Noch E, Yendamuri S, et al. Human microRNA genes are frequently located at fragile sites and genomic regions involved in cancers. *Proc Natl Acad Sci U S A* 2004;101:2999-3004.
17. Gupta RA, Shah N, Wang KC, Kim J, Horlings HM, Wong DJ, et al. Long non-coding RNA HOTAIR reprograms chromatin state to promote cancer metastasis. *Nature* 2010;464:1071-6.
18. Luthra R, Singh RR, Luthra MG, Li YX, Hannah C, Romans AM, et al. MicroRNA-196a targets annexin A1: a microRNA-mediated mechanism of annexin A1 downregulation in cancers. *Oncogene* 2008;27:6667-78.
19. Yekta S, Shih IH, Bartel DP. MicroRNA-directed cleavage of HOXB8 mRNA. *Science* 2004;304:594-6.
20. Rinn JL, Kertesz M, Wang JK, Squazzo SL, Xu X, Bruggmann SA, et al. Functional demarcation of active and silent chromatin domains in human HOX loci by noncoding RNAs. *Cell* 2007;129:1311-23.
21. Rink L, Skorobogatko Y, Kossenkov AV, Belinsky MG, Pajak T, Heinrich MC, et al. Gene expression signatures and response to imatinib mesylate in gastrointestinal stromal tumor. *Mol Cancer Ther* 2009;8:2172-82.
22. Maru DM, Singh RR, Hannah C, Albarracin CT, Li YX, Abraham R, et al. MicroRNA-196a is a potential marker of progression during Barrett's metaplasia-dysplasia-invasive adenocarcinoma sequence in esophagus. *Am J Pathol* 2009;174:1940-8.
23. Bloomston M, Frankel WL, Petrocca F, Volinia S, Alder H, Hagan JP, et al. MicroRNA expression patterns to differentiate pancreatic adenocarcinoma from normal pancreas and chronic pancreatitis. *JAMA* 2007;297:1901-8.
24. Guan Y, Mizoguchi M, Yoshimoto K, Hata N, Shono T, Suzuki SO, et al. MiRNA-196 is upregulated in glioblastoma but not in anaplastic astrocytoma and has prognostic significance. *Clin Cancer Res* 2010;16:4289-97.
25. Mueller DW, Bosserhoff AK. MicroRNA miR-196a controls melanoma-associated genes by regulating HOX-C8 expression. *Int J Cancer* 2011;129:1064-74.
26. Li Y, Zhang M, Chen H, Dong Z, Ganapathy V, Thangaraju M, et al. Ratio of miR-196s to HOXC8 messenger RNA correlates with breast cancer cell migration and metastasis. *Cancer Res* 2010;70:7894-904.
27. Shah N, Sukumar S. The Hox genes and their roles in oncogenesis. *Nat Rev Cancer* 2010;10:361-71.
28. Waitregny D, Alami Y, Clausse N, de Leval J, Castronovo V. Overexpression of the homeobox gene HOXC8 in human prostate cancer correlates with loss of tumor differentiation. *Prostate* 2002;50:162-9.
29. Miller GJ, Miller HL, van Bokhoven A, Lambert JR, Werahera PN, Schirripa O, et al. Aberrant HOXC expression accompanies the malignant phenotype in human prostate. *Cancer Res* 2003;63:5879-88.
30. Kikugawa T, Kinugasa Y, Shiraishi K, Nanba D, Nakashiro K, Tanji N, et al. PLZF regulates Pbx1 transcription and Pbx1-HoxC8 complex leads to androgen-independent prostate cancer proliferation. *Prostate* 2006;66:1092-9.
31. Alami Y, Castronovo V, Belotti D, Flagiello D, Clausse N. HOXC5 and HOXC8 expression are selectively turned on in human cervical cancer cells compared to normal keratinocytes. *Biochem Biophys Res Commun* 1999;257:738-45.
32. Zhai Y, Kuick R, Nan B, Ota I, Weiss SJ, Trimble CL, et al. Gene expression analysis of preinvasive and invasive cervical squamous cell carcinomas identifies HOXC10 as a key mediator of invasion. *Cancer Res* 2007;67:10163-72.
33. Braig S, Mueller DW, Rothhammer T, Bosserhoff AK. MicroRNA miR-196a is a central regulator of HOX-B7 and BMP4 expression in malignant melanoma. *Cell Mol Life Sci* 2010;67:3535-48.
34. Mueller DW, Bosserhoff AK. MicroRNA miR-196a controls melanoma-associated genes by regulating HOX-C8 expression. *Int J Cancer* 2011;129:1064-74.
35. Mansfield JH, Harfe BD, Nissen R, Obenaus J, Srineel J, Chaudhuri A, et al. MicroRNA-responsive 'sensor' transgenes uncover Hox-like and other developmentally regulated patterns of vertebrate microRNA expression. *Nat Genet* 2004;36:1079-83.
36. Tsai MC, Manor O, Wan Y, Mosammamaparast N, Wang JK, Lan F, et al. Long noncoding RNA as modular scaffold of histone modification complexes. *Science* 2010;329:689-93.
37. Yang Z, Zhou L, Wu LM, Lai MC, Xie HY, Zhang F, et al. Overexpression of long non-coding RNA HOTAIR predicts tumor recurrence in hepatocellular carcinoma patients following liver transplantation. *Ann Surg Oncol* 2011;18:1243-50.
38. Okada Y, Feng Q, Lin Y, Jiang Q, Li Y, Coffield VM, et al. hDOT1L links histone methylation to leukemogenesis. *Cell* 2005;121:167-78.
39. Krivtsov AV, Feng Z, Lemieux ME, Faber J, Vempati S, Sinha AU, et al. H3K79 methylation profiles define murine and human MLL-AF4 leukemias. *Cancer Cell* 2008;14:355-68.
40. Popovic R, Riesbeck LE, Velu CS, Chaubey A, Zhang J, Achille NJ, et al. Regulation of mir-196b by MLL and its overexpression by MLL fusions contributes to immortalization. *Blood* 2009;113:3314-22.
41. Hui AB, Shi W, Boutros PC, Miller N, Pintilie M, Fyles T, et al. Robust global micro-RNA profiling with formalin-fixed paraffin-embedded breast cancer tissues. *Lab Invest* 2009;89:597-606.



## Genome-wide Profiling of Chromatin Signatures Reveals Epigenetic Regulation of MicroRNA Genes in Colorectal Cancer

Hiromu Suzuki<sup>1,2</sup>, Shintaro Takatsuka<sup>3</sup>, Hirofumi Akashi<sup>3</sup>, Eiichiro Yamamoto<sup>1,2</sup>, Masanori Nojima<sup>4</sup>, Reo Maruyama<sup>1</sup>, Masahiro Kai<sup>1</sup>, Hiro-o Yamano<sup>6</sup>, Yasushi Sasaki<sup>5</sup>, Takashi Tokino<sup>5</sup>, Yasuhisa Shinomura<sup>2</sup>, Kohzoh Imai<sup>7</sup>, and Minoru Toyota<sup>1</sup>

### Abstract

Altered expression of microRNAs (miRNA) occurs commonly in human cancer, but the mechanisms are generally poorly understood. In this study, we examined the contribution of epigenetic mechanisms to miRNA dysregulation in colorectal cancer by carrying out high-resolution ChIP-seq. Specifically, we conducted genome-wide profiling of trimethylated histone H3 lysine 4 (H3K4me3), trimethylated histone H3 lysine 27 (H3K27me3), and dimethylated histone H3 lysine 9 (H3K9me2) in colorectal cancer cell lines. Combining miRNA expression profiles with chromatin signatures enabled us to predict the active promoters of 233 miRNAs encoded in 174 putative primary transcription units. By then comparing miRNA expression and histone modification before and after DNA demethylation, we identified 47 miRNAs encoded in 37 primary transcription units as potential targets of epigenetic silencing. The promoters of 22 transcription units were associated with CpG islands (CGI), all of which were hypermethylated in colorectal cancer cells. DNA demethylation led to increased H3K4me3 marking at silenced miRNA genes, whereas no restoration of H3K9me2 was detected in CGI-methylated miRNA genes. DNA demethylation also led to upregulation of H3K4me3 and H3K27me3 in a number of CGI-methylated miRNA genes. Among the miRNAs we found to be dysregulated, many of which are implicated in human cancer, miR-1-1 was methylated frequently in early and advanced colorectal cancer in which it may act as a tumor suppressor. Our findings offer insight into the association between chromatin signatures and miRNA dysregulation in cancer, and they also suggest that miRNA reexpression may contribute to the effects of epigenetic therapy. *Cancer Res*; 71(17); 5646–58. ©2011 AACR.

### Introduction

MicroRNAs (miRNA) are a class of small noncoding RNAs that regulate gene expression by inducing translational inhibition or direct degradation of target mRNAs through base pairing to partially complementary sites (1). miRNA genes are transcribed as large precursor RNAs, called pri-miRNAs, which may encode multiple miRNAs in a polycistronic arrange-

ment. The pri-miRNAs are then processed by the RNase III enzyme Drosha and its cofactor Patha to produce approximately 70-nucleotide hairpin structured second precursors (pre-miRNAs). The pre-miRNAs are then transported to the cytoplasm and processed by another RNase III enzyme, Dicer, to generate mature miRNA products. miRNAs are highly conserved among species and play critical roles in a variety of biological processes, including development, differentiation, cell proliferation, and apoptosis. Subsets of miRNAs are thought to act as tumor suppressor genes (TSG) or oncogenes, and their dysregulation is a common feature of human cancers (2). More specifically, expression of miRNAs is generally down-regulated in tumor tissues, as compared with the corresponding normal tissues, which suggests that some miRNAs may behave as TSGs in some tumors. Although the mechanism underlying the alteration of miRNA expression in cancer is still not fully understood, recent studies have shown that multiple mechanisms involved in regulating miRNA levels are affected in cancer. For example, genetic mutations that affect proteins involved in the processing and maturation of miRNA can lead to overall reductions in miRNA expression levels (3, 4). In addition, genetic and epigenetic alterations can disrupt expression of specific miRNAs in cancer.

**Authors' Affiliations:** <sup>1</sup>Department of Molecular Biology, <sup>2</sup>First Department of Internal Medicine, <sup>3</sup>Scholarly Information Center, <sup>4</sup>Department of Public Health, and <sup>5</sup>Medical Genome Science, Research Institute for Frontier Medicine, Sapporo Medical University, Sapporo; <sup>6</sup>Department of Gastroenterology, Akita Red Cross Hospital, Akita; and <sup>7</sup>Division of Novel Therapy for Cancer, The Advanced Clinical Research Center, The Institute of Medical Science, The University of Tokyo, Tokyo, Japan

**Note:** Supplementary data for this article are available at Cancer Research Online (<http://cancerres.aacrjournals.org/>).

**Corresponding Author:** Hiromu Suzuki, Department of Molecular Biology, Sapporo Medical University, S1, W17, Chuo-Ku, Sapporo 060-8556, Japan. Phone: 81-11-611-2111; Fax: 81-11-622-1918; E-mail: [hsuzuki@sapmed.ac.jp](mailto:hsuzuki@sapmed.ac.jp)

doi: 10.1158/0008-5472.CAN-11-1076

©2011 American Association for Cancer Research.



Epigenetic gene silencing due to promoter CpG island (CGI) hypermethylation is one of the most common mechanisms by which TSGs are inactivated during tumorigenesis. In recent years, it has become evident that some miRNA genes are also targets of epigenetic silencing in cancer. Others and we have previously shown that pharmacologic or genetic disruption of DNA methylation in cancer cell lines induces upregulation of substantial numbers of miRNAs (5, 6). These analyses led to identification of candidate tumor-suppressive miRNAs whose silencing was associated with CGI methylation. For example, miR-127 is embedded in a typical CGI, and treatment of human bladder cancer cells with inhibitors of histone deacetylase (HDAC) and DNA methyltransferase (DNMT) induced CGI demethylation and reexpression of the miRNA (7). In addition, methylation of miR-124 family members (miR-124-1, -124-2, and -124-3) was identified in colorectal cancer and was subsequently reported in tumors of other origins (5). Similarly, we found frequent methylation and downregulation of miR-34b/c in both colorectal cancer and gastric cancer (6, 8).

Epigenetic regulation of miRNA genes is tightly linked to chromatin signatures. For instance, transcriptionally active miRNA genes are characterized by active chromatin marks, such as trimethylated histone H3 lysine 4 (H3K4me3; ref. 9). We previously showed that restoring H3K4me3 through DNA demethylation could be a useful marker for predicting the promoter region of a silenced miRNA gene (6). However, the chromatin signatures, including both active and repressive histone marks on miRNA genes, within the cancer genome are still largely unknown. In the present study, we carried out genome-wide profiling of chromatin signatures in colorectal cancer cells and identified the active promoter regions of miRNA genes. We also show that changes in chromatin signatures before and after the removal of DNA methylation lead to robust identification of miRNA genes that are epigenetically regulated in cancer.

## Materials and Methods

### Cell lines and tissue specimens

Colorectal cancer cell lines and HCT116 cells harboring genetic disruptions within the *DNMT1* and *DNMT3B* loci [double knockout (DKO)] have been described previously (6). Treatment of cells with 5-aza-2'-deoxycytidine (DAC; Sigma-Aldrich) and 4-phenylbutyrate (PBA; Sigma-Aldrich) was carried out as described (8). A total of 90 primary colorectal cancer specimens were obtained as described (6, 10). Samples of adjacent normal colorectal mucosa were also collected from 20 patients. A total of 78 colorectal adenoma specimens were obtained through endoscopic biopsy. Informed consent was obtained from all patients before collection of the specimens. Total RNA from normal colonic mucosa from healthy individuals was purchased from Ambion. Total RNA was extracted using a mirVana miRNA isolation kit (Ambion) or TRIzol reagent (Invitrogen). Genomic DNA was extracted using the standard phenol-chloroform procedure.

### miRNA expression profiling

Expression of 470 miRNAs was analyzed using Human miRNA Microarray V1 (G4470A; Agilent Technologies) as described previously (8). In addition, expression of 664 miRNAs was analyzed using a TaqMan microRNA Array v2.0 (Applied Biosystems). Briefly, 1  $\mu$ g of total RNA was reverse transcribed using Megaplex Pools kit (Applied Biosystems), after which the miRNAs were amplified and detected using PCR with specific primers and TaqMan probes. The PCR was run in a 7900HT Fast Real-Time PCR system (Applied Biosystems), and SDS2.2.2 software (Applied Biosystems) was used for comparative  $\Delta C_t$  analysis. U6 snRNA (RNU6B; Applied Biosystems) served as an endogenous control. Microarray data and TaqMan Array data ( $\Delta C_t$  values) were further analyzed using GeneSpring GX ver. 11 (Agilent Technologies). The Gene Expression Omnibus accession number for the microarray data is GSE29900.

### Real-time reverse transcriptase PCR of miRNA

Expression of selected miRNAs was analyzed using TaqMan microRNA Assays (Applied Biosystems). Briefly, 5 ng of total RNA was reverse transcribed using specific stem-loop RT primers, after which the miRNAs were amplified and detected using PCR with specific primers and TaqMan probes as described earlier. U6 snRNA (RNU6B) served as an endogenous control. Expression of the primary miR-1-1 transcript was analyzed using a TaqMan Pri-miRNA assay (assay ID Hs03303345\_pri; Applied Biosystems). Glyceraldehyde-3-phosphate dehydrogenase (GAPDH; assay ID Hs99999905\_m1; Applied Biosystems) served as an endogenous control.

### Chromatin immunoprecipitation-on-chip analysis

Chromatin immunoprecipitation (ChIP)-on-chip analysis was carried out according to Agilent Mammalian ChIP-on-chip Protocol version 10.0 (Agilent Technologies). Briefly,  $1 \times 10^8$  cells were treated with 1% formaldehyde for 10 minutes to cross-link histones with the DNA. After washing with PBS, the cell pellets were resuspended in 3 mL of lysis buffer and sonicated. Chromatin was immunoprecipitated for 16 hours at 4°C using 10  $\mu$ L of anti-trimethyl histone H3K4 (clone MC315; Upstate), anti-trimethyl histone (clone H3K27; Upstate) or anti-dimethyl histone H3K79 (clone NL59; Upstate) antibody. Before adding antibodies, 50  $\mu$ L of the each cell lysate was saved as an internal control for the input DNA. After washing, elution, and reversal of the cross-links, input DNA and the immunoprecipitate were ligated to linkers and PCR amplified. Input DNA and the immunoprecipitate were then labeled with Cy3 and Cy5 using an Agilent Genomic DNA Enzymatic Labeling kit (Agilent Technologies) and hybridized to the 244K Human Promoter ChIP-on-chip microarray (G4489A; Agilent technologies). After washing, the array was scanned using an Agilent DNA Microarray scanner (Agilent Technologies), and the data were processed using Feature Extraction software (Agilent Technologies).

### ChIP-seq analysis

ChIP experiments were carried out as described earlier, after which massively parallel sequencing was carried out



using a SOLiD3 Plus system (Applied Biosystems) according to the manufacturer's instructions. Briefly, 100 ng of input DNA or the immunoprecipitate was ligated to adapters and PCR amplified using a SOLiD Fragment Library Construction kit (Applied Biosystems). Template bead preparation was carried out using a SOLiD ePCR kit V2 (Applied Biosystems) and a SOLiD Bead Enrichment kit (Applied Biosystems). Approximately 40 to 50 million beads per sample were sequenced using SOLiD Opti Fragment Library Sequencing Master Mix 50 (Applied Biosystems) and a SOLiD3 Plus sequencer (Applied Biosystems). Sequence reads that were of poor quality or those that were not uniquely mapped were excluded from the study. Peaks were identified using the Model-based Analysis for ChIP-seq (MACS) software (11) and visualized using the University of California Santa Cruz (UCSC) genome browser.

#### Reference sequence

Genomic locations are based on the UCSC hg18 (National Center for Biotechnology Information Build 36.1, March 2006), which was produced by the International Human Genome Sequencing Consortium. We also obtained locations of CGIs, ReSeq genes, and UCSC genes from the UCSC hg18 data sets.

#### Methylation analysis

Genomic DNA (2  $\mu$ g) was modified with sodium bisulfite using an EpiTect Bisulfite kit (QIAGEN). Methylation-specific PCR (MSP), bisulfite sequencing, and bisulfite pyrosequencing were carried out as described (6). For bisulfite sequencing analysis, amplified PCR products were cloned into pCR2.1-TOPO vector (Invitrogen), and 10 to 12 clones from each sample were sequenced using an ABI3130x automated sequencer (Applied Biosystems). Primer sequences and PCR product sizes are listed in Supplementary Table S1.

#### Transfection of miRNA precursor molecules

Colorectal cancer cells ( $1 \times 10^6$  cells) were transfected with 100 pmol of Pre-miRNA miRNA Precursor Molecules (Ambion) or Pre-miRNA miRNA Molecules Negative Control #1 (Ambion) using a Cell Line Nucleofector kit V (Lonza) with a Nucleofector I electroporation device (Lonza) according to the manufacturer's instructions. Total RNA or cell lysate was extracted 48 hours after transfection. Cell viability assays, Western blotting, wound-healing assays, and Matrigel invasion assays are described in the Supplementary Methods.

#### Gene expression profiling

Total RNA (700 ng) was amplified and labeled using a Quick Amp Labeling kit one-color (Agilent Technologies), after which the synthesized cRNA was hybridized to the Whole Human Genome Oligo DNA microarray (G4112F; Agilent technologies). Data analysis was carried out using GeneSpring GX ver. 11 (Agilent technologies). The Gene Expression Omnibus accession number for the microarray data is GSE29760.

#### miRNA target predictions and luciferase reporter assays

The predicted targets of miR-1 and their downstream target sites were analyzed using TargetScan and miRanda. Construc-

tion of luciferase reporter vectors containing the predicted target sites and dual luciferase reporter assays were carried out as described in Supplementary Methods.

## Results

### miRNA profiling in colorectal cancer cell lines

To screen for epigenetically silenced miRNAs, we first carried out miRNA microarray analysis in a series of colorectal cancer cell lines (HCT116, DLD1, and RKO) and normal colonic tissue. Hierarchical clustering analysis revealed that expression of a majority of miRNAs was downregulated in all 3 colorectal cancer cell lines tested, as compared with normal colonic mucosa (Supplementary Fig. S1A). DAC treatment upregulated expression of a large number of miRNAs in all 3 colorectal cancer cell lines (Supplementary Fig. S1B), and combination treatment with DAC plus PBA induced even greater numbers of miRNAs in colorectal cancer cells (Supplementary Fig. S1C and D). However, the most profound effect on the miRNA expression profile was induced by genetic disruption of *DNMT1* and *DNMT3B* in HCT116 cells (DKO cells; Supplementary Fig. S1C). We also noted a novel overlap between miRNAs upregulated by pharmacologic or genetic disruption of DNA methylation and those downregulated in colorectal cancer cells, as compared with normal colonic mucosa (Supplementary Fig. S1E-G). To test the tumor-suppressive potentials of the downregulated miRNAs, we constructed expression vectors encoding selected miRNAs and carried out colony formation assays. We found that a majority of miRNAs exerted growth-suppressive effects when they were ectopically expressed in colorectal cancer cells (Supplementary Fig. S2). These results suggest that an epigenetic mechanism plays an essential role in the downregulation of a number of miRNAs in cancer and that such downregulation of numerous miRNAs may contribute to tumorigenesis.

### Chromatin signatures of active and silenced miRNA genes

We next examined the chromatin signatures of miRNA genes in HCT116 colorectal cancer cells, with and without genetic disruption of *DNMT1* and *DNMT3B* (DKO cells). We carried out ChIP analysis using antibodies against trimethylated histone H3 lysine 4 (H3K4me3), which marks active promoters; dimethylated histone H3 lysine 79 (H3K79me2), which is associated with transcriptional elongation; and trimethylated histone H3 lysine 27 (H3K27me3), which is a repressive mark. We started our analysis using the Agilent 244K Promoter Array, which covers approximately 370 human miRNA genes, and we subsequently migrated to ChIP-seq analysis to increase our scope within the genome. We observed a good correlation between the results of the ChIP-on-chip and ChIP-seq analyses (Supplementary Fig. S3). We also validated the reliability of our ChIP-seq data by checking representative protein-coding genes that were transcriptionally active or silenced in HCT116 cells (Supplementary Fig. S4).

Representative chromatin signatures of miRNA genes are shown in Fig. 1A. We found enrichment of the H3K4me3 mark around the proximal upstream CGI regions of 2 abundantly

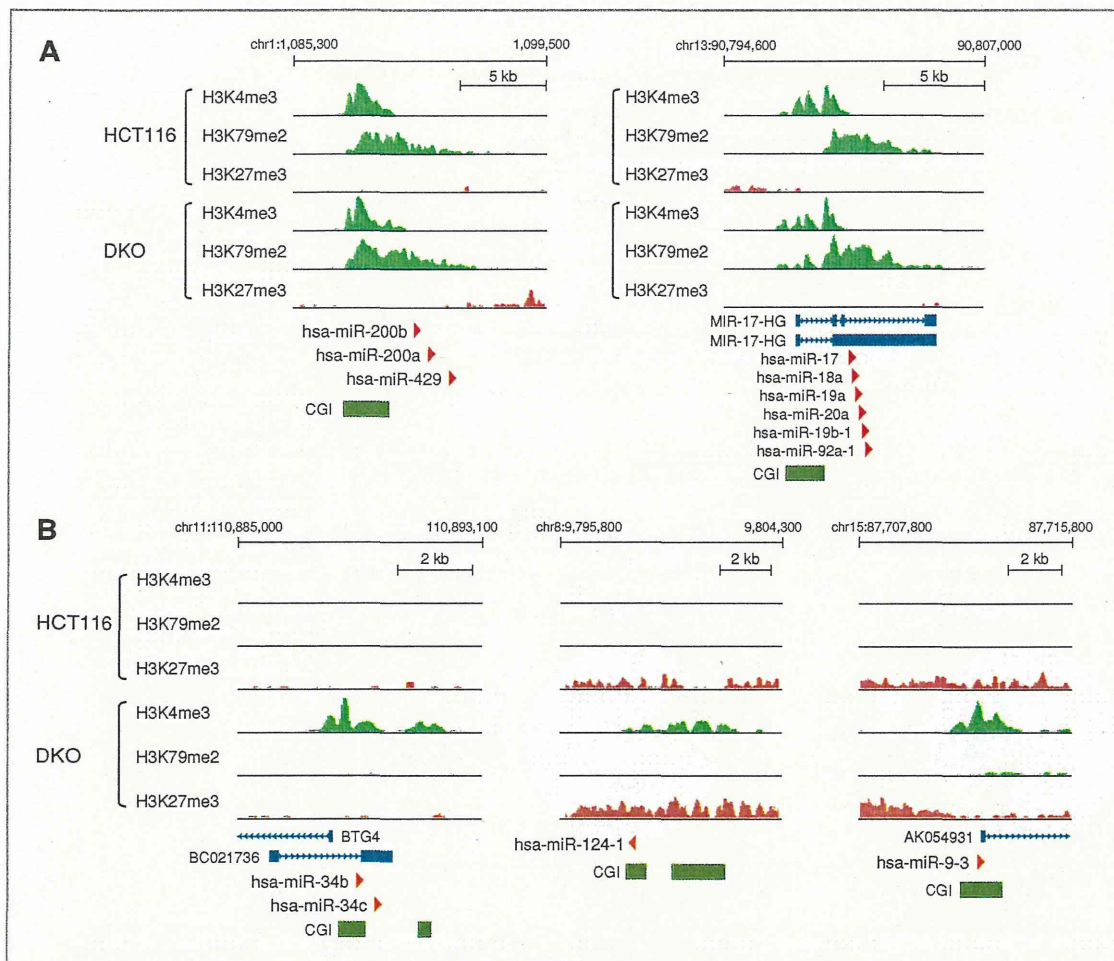


Figure 1. Chromatin signatures of transcriptionally active and epigenetically silenced miRNA genes in colorectal cancer. A, ChIP-seq results for H3K4me3, H3K79me2, and H3K27me3 in transcriptionally active miRNA genes in HCT116 and DKO cells. Chromosomal locations are indicated on the top. Locations of host genes, pre-miRNA genes, and CGIs are shown below. B, ChIP-seq results for epigenetically silenced miRNAs with associated CGI hypermethylation. CGI methylation is lost and miRNAs are reexpressed in DKO cells. H3K4me3 marking is upregulated in the putative promoter regions in DKO cells, whereas H3K79me2 shows only a minimal increase.

expressed miRNA clusters, miR-200b and miR-17, in both wild-type HCT116 and DKO cells (Fig. 1A). Gene bodies were marked by H3K79me2, which indicates active transcriptional elongation, whereas they almost completely lacked the repressive H3K27me3 mark. With respect to the H3K4me3 mark in the miR-17 cluster, we observed a sharp dip at the transcription start site (TSS) of the host gene and another dip downstream, which is consistent with a previous report that miR-17 has its own TSS within the intron of the host gene (Fig. 1A; ref. 12).

In contrast, miRNAs whose silencing was associated with promoter CGI hypermethylation completely lacked both of the active histone marks. The CGIs of miR-34b/c, miR-124-1, and miR-9-3 were densely methylated in HCT116 cells (5, 6,

13) and were completely devoid of H3K4me3 and H3K79me2 marks (Fig. 1B). miR-124-1 and miR-9-3 showed moderate enrichment of H3K27me3, whereas miR-34b/c was almost H3K27me3 free, which corresponds to previous reports that DNA methylation and H3K27me3 are sometimes observed independently in cancer (14). In DKO cells, where DNA methylation was significantly diminished and gene expression was restored, increased H3K4me3 marks were found at the upstream CGI, though restoration of H3K79me2 was quite limited. Upregulation of H3K27me3 was also seen around miR-124-1 and miR-9-3, which is consistent with previous observations that genes with methylated CGIs adopt a bivalent chromatin pattern after DNA demethylation (15, 16).



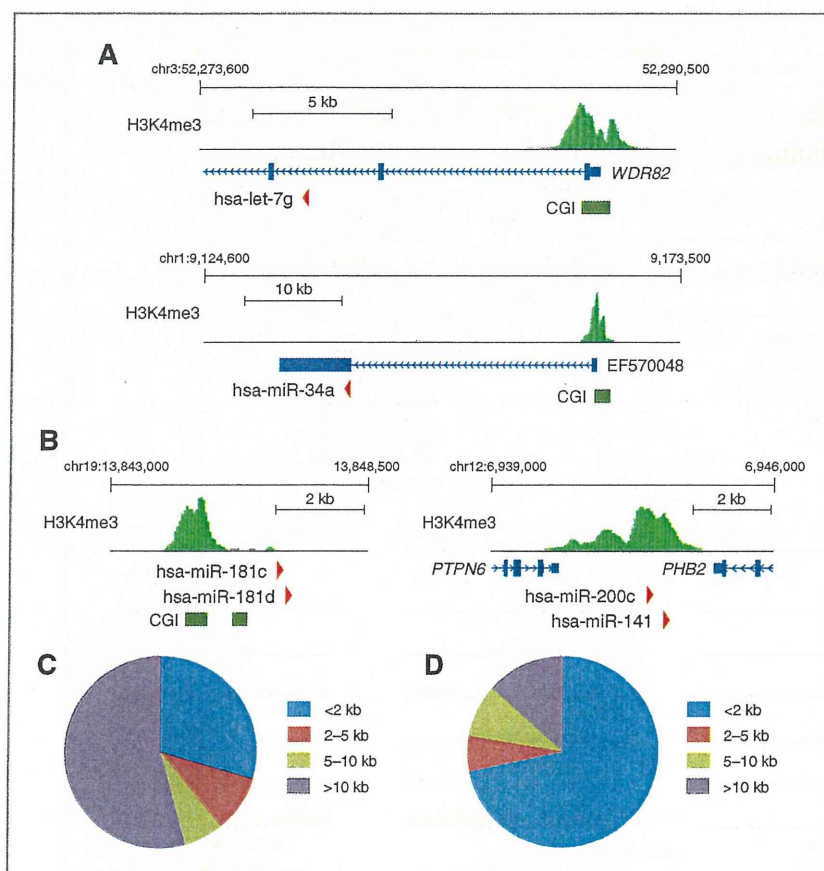


Figure 2. Identification of miRNA gene promoter regions using chromatin signatures. A, examples of H3K4me3 marks in intragenic miRNAs. Let-7g is located within the intron of the protein-coding gene *WDR82*, and miR-34a is located within the exon of a noncoding host gene. H3K4me3 marks are observed in the TSS regions of the host genes, suggesting that these miRNAs share common promoters with their host genes. B, examples of H3K4me3 marking of intergenic miRNA genes. C, summarized distances between intragenic pre-miRNA coding regions and their putative promoter regions ( $n = 166$ ). D, summarized distances between intergenic pre-miRNA coding regions and their putative promoter regions ( $n = 67$ ).

#### Identification of putative miRNA promoter regions

Identification of epigenetically silenced miRNAs is sometimes hampered by a lack of knowledge of the transcription initiation region of the primary miRNA transcripts. Previous studies have shown that H3K4me3 is a useful marker for identifying active miRNA gene promoters (9, 12), and we employed that approach with colorectal cancer cells. Using miRNA microarrays and TaqMan low-density arrays, we detected expression of 339 and 429 distinct mature miRNAs in HCT116 and DKO cells, respectively. We then searched for the putative promoter regions of these miRNAs, using H3K4me3 as a marker.

More than half of miRNAs are located in the introns of protein-coding or long noncoding RNA genes, and it is generally believed that intragenic miRNAs share common promoters with their host genes (17). We identified the putative promoters of 166 intragenic miRNAs located in RefSeq genes and/or UCSC genes, and a majority of the H3K4me3 marks were observed at the TSS of the host genes, many of which were located more than 10 kb upstream of the pre-miRNA coding regions (Fig. 2A and C, Supplementary Fig. S5A, and Supplementary Table S2). In contrast, intragenic H3K4me3

marks were identified in the proximal upstream of 22 pre-miRNAs, indicating these miRNAs have their own promoters and are transcribed independently of their host genes (Supplementary Fig. S6, Supplementary Table S3). To identify promoters of intergenic miRNAs, we first searched 10 kb upstream for H3K4me3 marks and also explored the initiation sites of overlapping 5' expressed sequence tags (EST). We identified the putative promoters of 66 intergenic miRNAs, the majority of which (47 of 66) were identified in the proximal upstream (<2 kb) of the pre-miRNA coding region (Fig. 2B and D, Supplementary Fig. S5B, and Supplementary Table S2). In total, we identified the putative promoters of 174 transcript units encoding 233 distinct pre-miRNAs, whereas promoters of 135 miRNAs remain unidentified, despite their positive expression in colorectal cancer cells.

We validated our promoter search by comparing our results with previously reported transcription initiation regions. Promoters of 177 pre-miRNAs that we identified overlapped with those identified in human embryonic stem (ES) cells by Marson and colleagues (9), whereas only the promoters of 38 pre-miRNAs did not match. Similarly, the TSS of 65 miRNAs identified in human melanoma and breast cancer cell lines by

Ozsolak and colleagues overlapped with the promoters we identified (12). For example, we found H3K4me3 marks overlapping with known TSS of the miR-17 cluster, *let-7a-1/let-7f-1/let-7d*, and miR-200c/141 (Fig. 2B, Supplementary Fig. S5). We also identified an H3K4me3 mark at the intronic transcription initiating region of miR-21 (Supplementary Fig. S6C). The high degree of consistency between our results and those of earlier studies attests to the accuracy of our promoter prediction.

#### Identification of epigenetically silenced miRNAs

We next endeavored to identify epigenetically silenced miRNA genes by taking advantage of the observation that DNA demethylation can induce increases in H3K4me3 in the

promoters of the epigenetically silenced genes (6). We searched for miRNA genes showing reduction or loss of both expression and H3K4me3 marks in HCT116 and DKO cells. We identified 47 pre-miRNA genes encoded in 37 primary transcription units as potential targets of epigenetic silencing in HCT116 cells. Promoters of 22 transcription units were associated with CGIs, and MSP analysis revealed that all of the CGIs were methylated (Fig. 3A and B, Table 1). In most cases, DNA demethylation led to increases in H3K4me3 and H3K27me3 marking of the methylated CGIs of miRNA genes, whereas H3K79me2 marks were not restored by demethylation (Fig. 3C). In contrast, the chromatin signatures of miRNAs without promoter CGIs were more variable among genes. We

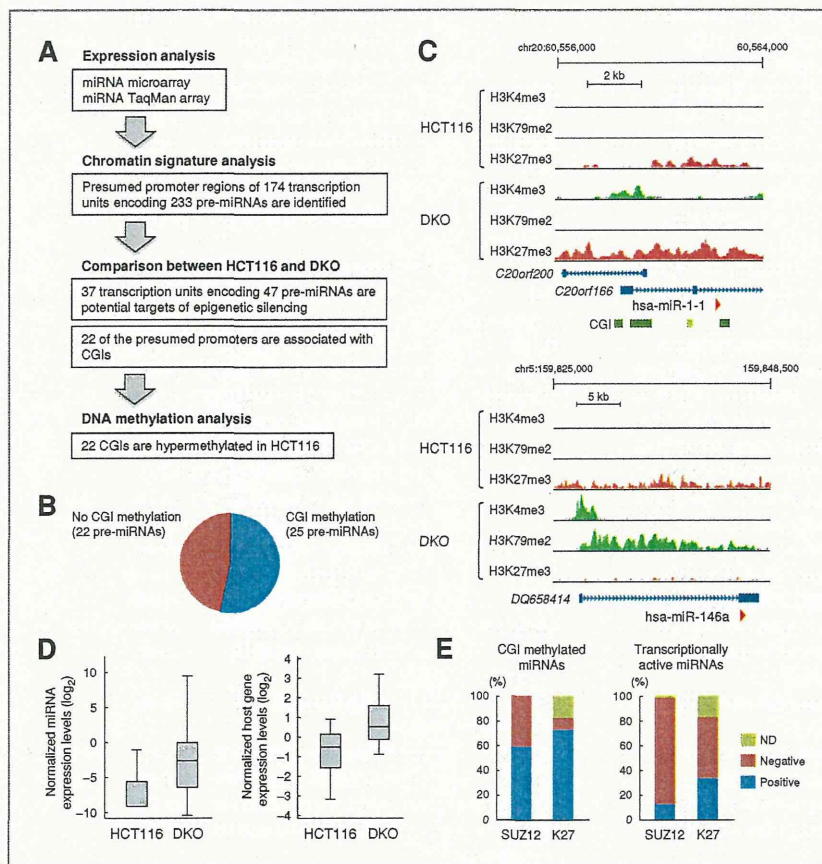


Figure 3. Identification of epigenetically silenced miRNA genes. A, flowchart for the selection of epigenetically silenced miRNA genes in colorectal cancer. B, graph showing the number of epigenetically silenced miRNAs associated with CGI methylation and those without CGI methylation. C, chromatin signatures of 2 representative miRNA genes, with and without promoter CGI methylation. miR-1-1 (top) was silenced in association with CGI methylation in HCT116 cells. In DKO cells, H3K4me3 marking was observed around the transcription start site of the host gene *C20orf166*. miR-146a (bottom) is another candidate target for epigenetic silencing in HCT116, though its promoter is not associated with CGI. Both H4K4me3 and H3K79me2 were restored in DKO cells. D, expression levels of epigenetically silenced miRNAs and their host genes in HCT116 and DKO cells. TaqMan real-time PCR data for 57 mature miRNAs encoded by 47 pre-miRNA genes were imported into Gene Spring GX, after which the data were normalized and shown in box plots (left). Expression data of 13 host genes of epigenetically silenced miRNAs were obtained using an Agilent Whole Human Genome microarray (right). E, miRNAs targeted by the PcG group in ES cells are more likely to be silenced by CGI hypermethylation in colorectal cancer cells. CGI-methylated miRNAs ( $n = 22$ ; left) or transcriptionally active miRNAs ( $n = 146$ ; right) were selected, and their SUZ12 binding and H3K27me3 enrichment in human ES cells were assessed. Of 22 CGI-methylated miRNAs, 13 (59%) were positive for SUZ12 and 16 (73%) for H3K27me3. ND, not determined.